# Materials development and mid-infrared emission properties of Dy-doped TlPb2Br5 and CsPbCl3

Hömmerich, U., Hart, D., Kabir, A., Yang, C., Trivedi, S. B.

U. Hömmerich, D. Hart, A. Kabir, C. Yang, S. B. Trivedi, "Materials development and mid-infrared emission properties of Dy-doped TlPb2Br5 and CsPbCl3," Proc. SPIE 11276, Optical Components and Materials XVII, 112761D (3 March 2020); doi: 10.1117/12.2542697

SPIE.

Event: SPIE OPTO, 2020, San Francisco, California, United States

# Materials development and mid-infrared emission properties of Dy-doped $TlPb_2Br_5$ and $CsPbCl_3$

U. Hömmerich[a], D. Hart[a], A. Kabir[a], C. Yang[b], and S. B. Trivedi[b]
[a]Department of Physics, Hampton University, Hampton, VA 23668; [b]Brimrose Technology Corporation, Sparks Glencoe, MD 21152

## ABSTRACT

We report on the materials development and infrared (IR) optical spectroscopy of $Dy^{3+}$-doped into the ternary lead halides compounds $TlPb_2Br_5$ and $CsPbCl_3$ for photonic applications. The investigated Dy-doped ternary lead halides were synthesized from purified starting materials followed by melt-growth using vertical Bridgman technique. Under optical pumping at 1.35 µm ($^6H_{15/2}\rightarrow{}^6H_{9/2}+{}^6F_{11/2}$), broad mid-IR emissions in the ~2.9 µm ($^6H_{13/2}\rightarrow{}^6H_{15/2}$), ~4.3 µm ($^6H_{11/2}\rightarrow{}^6H_{13/2}$), and ~5.4 µm ($^6H_{9/2}+{}^6F_{11/2}\rightarrow{}^6H_{15/2}$) regions were observed at room-temperature. Compared to Dy: $TlPb_2Br_5$, the mid-IR emission from Dy: $CsPbCl_3$ was significantly weaker suggesting the existence of non-radiative losses. Temperature dependent lifetime studies and a Judd-Ofelt analysis were performed for Dy: $TlPb_2Br_5$.

**Keywords:** Rare earth doped crystals, $Dy^{3+}$ Spectroscopy, IR gain media, ternary halide perovskite

## 1. INTRODUCTION

There is a continued interest in the development of lead halides perovskites and related compounds for a broad range of applications including photo-voltaic devices, nuclear radiation detection, visible lasers, and solid-state lighting [1-3]. Bulk crystals of binary and ternary lead chloride and bromide crystals have also been intensively studied as low-phonon energy hosts for rare earth (RE) doping leading to emissions in the mid-IR spectral region [4-8]. The narrow-phonon spectrum of lead halide based crystals results into reduced non-radiative decay rates between closely spaced RE energy levels with efficient emission and lasing at longer IR wavelengths. For example, RE doped $KPb_2Cl_5$ and $RbPb_2Cl_5$ crystals ($h\omega_{max}$~200 $cm^{-1}$) have shown IR lasing at ~4.4 µm [5], and 5.5 µm [6]. In this work, we present new results of the material preparation and spectroscopy for $Dy^{3+}$ doped $TlPb_2Br_5$ and $CsPbCl_3$ for mid-IR photonic applications. Spectroscopic measurements will be discussed including absorption and emission spectra as well as temperature dependent decay times. The resulting data were analyzed to derive transition wavelengths and cross-sections. A Judd-Ofelt analysis was performed for Dy: $TlPb_2Br_5$ to determine emission branching ratios and radiative decay rates.

## 2. MATERIALS AND EXPERIMENTAL DETAILS

Dy: $TlPb_2Br_5$ (Dy: TPB) and Dy: $CsPbCl_3$ (Dy: CPC) crystals were grown using in-house crystal growth facilities as described previously [7,8]. Briefly, undoped TPB and CPC materials were synthesized from high purity (5N) starting materials of $PbBr_2$, TlBr, and $PbCl_2$, CsCl, respectively. For rare earth doping, a nominal concentration of ~1-2 wt% of $DyBr_3$ and $DyCl_3$ were added to the purified TPB and CPC, respectively. The Dy: TPB and Dy: CPC crystals were subsequently melt-grown using vertical Bridgman technique employing a two zone furnace. Nearly crack-free material of Dy: TPB with good optical quality were selected from the middle part of the ingot and a sample of ~3 mm thickness was polished for spectroscopic measurements. The resulting Dy: CPC material was polycrystalline with poor optical transmission, but the sample was sufficient for initial IR emission spectroscopy.

Transmission and absorption spectra were measured using a Shimadzu UV-3600 spectrophotometer and Nicholet 6700 FTIR. The emission was excited using a modulated 1.35 µm fiber-coupled diode-laser. For mid-IR emission (2-5.5 µm) studies a 0.3 m spectrometer was employed with a grating blazed at 4 µm. The appropriate long pass filters were placed in front of the entrance slit of the spectrometer to block laser scattering. The emission signal was recorded using a liquid-nitrogen cooled InSb detector and spectra were recorded using a lockin amplifier. The mid-IR emission setup was carefully calibrated for the spectral response of the experimental setup. For emission lifetime studies a pulsed (10 Hz, 5-10 ns pulses) Optical Parametric Oscillator was used as pump sources. The decay transients were measured using

Optical Components and Materials XVII, edited by Shibin Jiang, Michel J. F. Digonnet,
Proc. of SPIE Vol. 11276, 112761D · © 2020 SPIE · CCC code: 0277-786X/20/$21
doi: 10.1117/12.2542697

appropriate bandpass filters and recorded with a digital oscilloscope. Temperature dependent lifetime studies were performed by mounting the sample on the cold finger of a closed-cycle helium refrigerator.

## 3. RESULTS AND DISCUSSION

### 3.1 IR Optical Spectroscopy and Judd-Ofelt Analysis for Dy: $TlPb_2Br_5$

The background corrected IR absorption cross-section spectrum of Dy: TPB is shown in Fig. 1. Intra-4f absorption bands originating from the $^6H_{15/2}$ ground state of $Dy^{3+}$ ions are indicated in the figure. The assignment of absorption transitions was made in close agreement with published data on other Dy doped crystals [4,6].

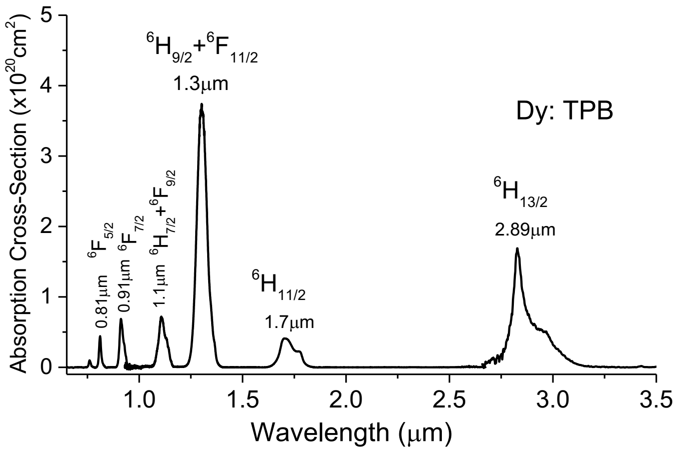


Figure 1. Background correction IR absorption cross-section spectrum of Dy: TPB at room temperature.

Dy: TPB exhibited several IR absorption bands suitable for optical pumping using commercially available diode/fiber lasers at ~0.8 μm ($^6H_{15/2} \rightarrow {}^6F_{5/2}$), ~1.3 μm ($^6H_{15/2} \rightarrow {}^6H_{9/2} + {}^6F_{11/2}$), and ~ 1.7 μm ($^6H_{15/2} \rightarrow {}^6H_{11/2}$). Using six $Dy^{3+}$ absorption bands a Judd-Ofelt (JO) analysis was performed and yielded the following intensity parameters for Dy: TPB: $\Omega_2$=10.44x10$^{-20}$ cm$^2$, $\Omega_4$=1.79x10$^{-20}$ cm$^2$, and $\Omega_6$=1.20x10$^{-20}$ cm$^2$. Magnetic dipole contributions were subtracted from the measured line strengths as needed [4,9].

Table I: Absorption transitions, average absorption wavelengths, integrated absorption coefficients, experimental line strengths, and calculated line strengths values for Dy: TPB.

| Transition $^6H_{15/2} \rightarrow$ | Average Wavelength (μm) | $\int \alpha (\lambda)\, d\lambda$ (μm/cm) | $S^{ed}$ (experimental) (x 10$^{-20}$ cm$^2$) | ($S^{ed}$ (calculated) (x 10$^{-20}$ cm$^2$) |
|---|---|---|---|---|
| $^6H_{13}$ | 2.89 | 0.678 | 3.58 | 3.87 |
| $^6H_{11/2}$ | 1.7 | 0.128 | 1.47 | 1.49 |
| $^6H_{9/2}+^6F_{11/2}$ | 1.3 | 0.739 | 11.21 | 11.13 |
| $^6H_{7/2}+^6F_{9/2}$ | 1.1 | 0.108 | 1.92 | 1.87 |
| $^6F_{7/2}$ | 0.91 | 0.054 | 1.17 | 1.01 |
| $^6F_{5/2}$ | 0.81 | 0.019 | 0.47 | 0.41 |

The room-temperature emission cross-section spectra and lifetimes for the 2.85 μm ($^6H_{13/2} \rightarrow {}^6H_{15/2}$), 4.33 μm ($^6H_{11/2} \rightarrow {}^6H_{13/2}$), and 5.41 μm ($^6H_{9/2} + {}^6F_{11/2} \rightarrow {}^6H_{15/2}$) bands for Dy: TPB are shown in Fig 2. The emission spectra were excited using a 1.35 μm fiber-coupled diode-lasers, whereas the lifetimes were excited using a pulsed laser operating at either 1.3 μm (for emission at ~2.9 μm & ~5.4 μm) or 1.7 μm (for emission at ~4.3 μm). The emission transients were nearly exponential with lifetime values of 11.1 ms, 3.9 ms, and ~0.1 ms for the 2.85, 4.33, and 5.42 μm bands, respectively. It can be noticed that the measured room-temperature lifetimes where longer compared to the calculated radiative decay times from the JO analysis for the $^6H_{13/2}$ and $^6H_{11/2}$ excited states (see Table 2) suggesting possible lifetime lengthening due to re-absorption [6]. Temperature dependent lifetime studies shown in Fig. 3 reveal a slight increase in lifetimes for the range from 12-300 K. It is noteworthy that the measured low temperature (12 K) lifetimes of the 2.85 μm and 4.33 μm emissions are in good agreement with the JO derived lifetimes as shown in Table II.

Additional lifetime studies of Dy: TPB samples with different geometries as well as powder samples are in progress to determine re-absorption effects. Based on the JO analysis and temperature dependent lifetime studies it can be concluded that non-radiative decay is negligible for the 2.85 μm and 4.33 μm emission bands of Dy: TPB and the emission quantum efficiencies are near unity at room-temperature. This conclusion is also consistent with non-radiative decay rate calculations assuming multi-phonon relaxations with a low-phonon energy of $h\omega \sim 140\ cm^{-1}$ and using host-dependent phenomenological parameters as published for $KPb_2Br_5$ [9,10].

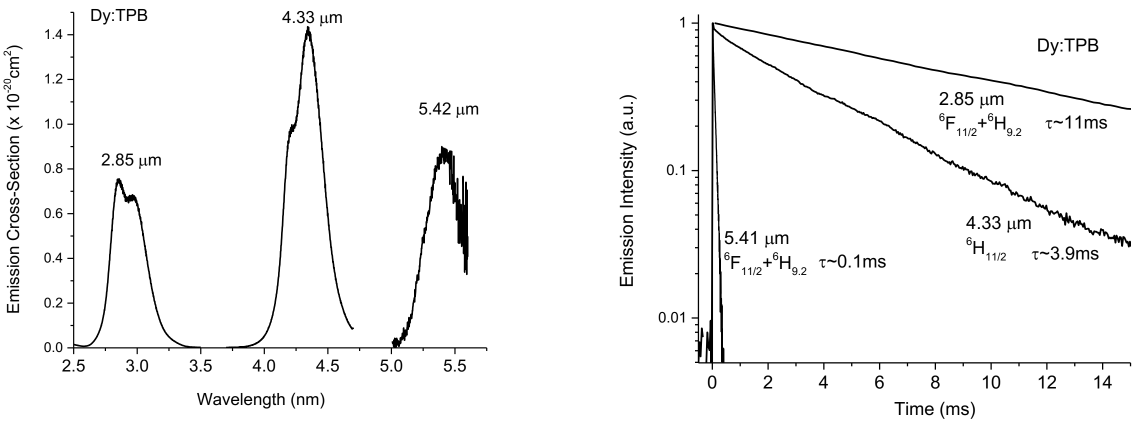


Figure 2. Mid-IR emission cross-section spectra (left) and lifetimes (right) for Dy: TPB at room-temperature. All emission spectra were recorded under 1.35 μm diode-laser pumping. The emission lifetime transients were measured under pulsed excitation at 1.35 μm (2.85μm & 5.41 μm bands) and 1.7 μm (4.33 μm band).

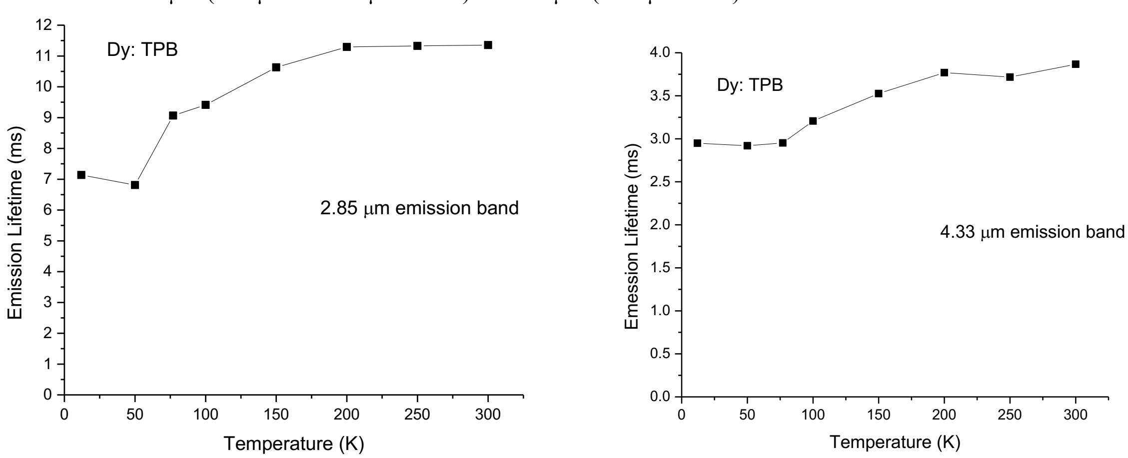


Figure 3. Temperature dependent lifetime studies for the 2.85 μm ($^6H_{13/2}$ level) and 4.33 μm ($^6H_{11/2}$ level) emission bands.

Table 2: Emission transitions, emission wavelengths, branching ratios, radiative lifetimes determined from a JO analysis, and experimental lifetimes for Dy: TPB at 300K.

| Initial State | Final State | $\lambda$ (μm) | $\beta_{ij}$ (%) | $\tau_{rad}$ (ms) | $\tau_{exp}$ (ms) |
|---|---|---|---|---|---|
| $^6H_{13/2}$ | $^6H_{15/2}$ | 2.85 | 1 | 7.8 | 11.1 |
| $^6H_{11/2}$ | $^6H_{13/2}$ | 4.33 | 15.8 | | |
| | $^6H_{15/2}$ | 1.7 | 84.2 | 3.4 | 3.9 |
| $^6H_{9/2}$+$^6F_{11/2}$ | $^6H_{11/2}$ | 5.42 | 0.6 | | |
| | $^6H_{13/2}$ | 2.4 | 6.3 | | |
| | $^6H_{15/2}$ | 1.3 | 93.1 | 0.4 | ~0.1 |

The decay dynamics of the 5 μm emission seems more complicated and the measured lifetime is significantly shorter compared to the radiative lifetime determined from the JO analysis with an estimated quantum efficiency of ~25% at room-temperature. It was also noted that under 1.3 μm pumping, Dy: TPB revealed a weak yellow emission indicating the existence of possible $Dy^{3+}$ upconversion processes [11]. Concentration dependent studies are needed to gain more insight in the decay dynamics of the $^6H_{9/2}$+$^6F_{11/2}$ excited state in Dy: TPB. Based on the existing spectroscopic data and results of the JO analysis the peak emission cross-sections were determined to be $0.76\times10^{-20}$ cm$^2$, $1.42\times10^{-20}$ cm$^2$, and $0.87\times10^{-20}$ cm$^2$ for the 2.85, 4.3, and 5.4 μm emission bands, respectively. These cross-sections compare favorably to other Dy based laser crystals and indicate the potential of Dy: TPB for mid-IR laser applications.

### 3.2 IR Emission Spectroscopy of Dy: $CsPbCl_3$

Fig. 4 shows initial mid-IR emission spectra of Dy: CPC recorded at room-temperature. Compared to Dy: TPB, the IR emissions from Dy: CPC were nearly two orders of magnitude weaker under similar experimental conditions. The emissions from the $^6H_{13/2}\rightarrow^6H_{15/2}$ and $^6H_{11/2}\rightarrow^6H_{13/2}$ transitions were located at ~2.8 μm and ~4.3 μm. The onset of the $^6H_{9/2}+^6F_{11/2}\rightarrow^6H_{11/2}$ emission band was observed at longer wavelength with an estimated peak at ~5.4 μm. The emission was truncated due to the end of InSb detector response.

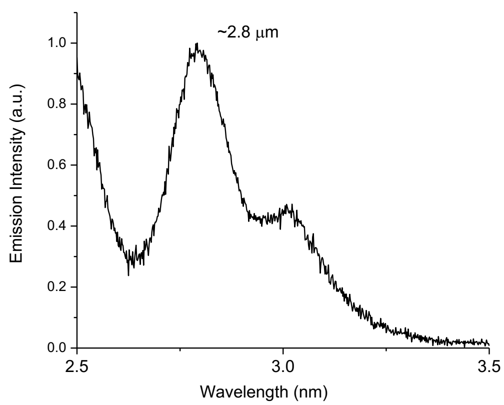


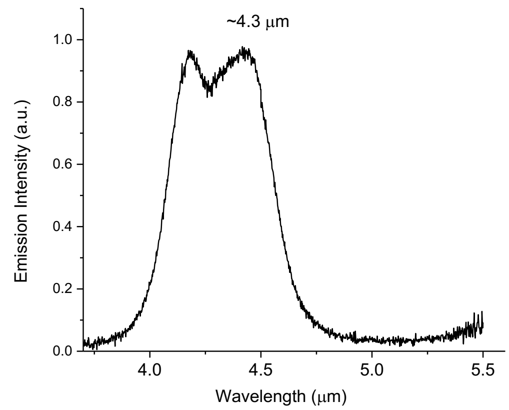


Figure 4. Normalized mid-IR emission spectra in the ~2.8 μm (left) and ~4.3 μm (right) spectral regions for Dy: CPC at room-temperature. The onset of a weak emission band can be noticed at ~5.4 μm.

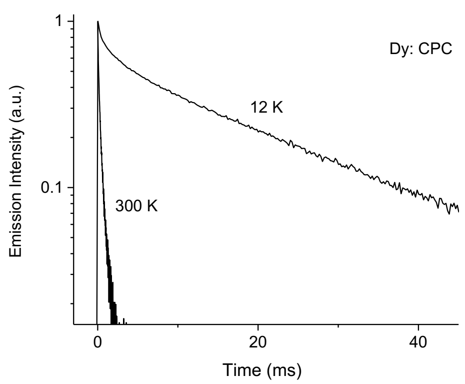


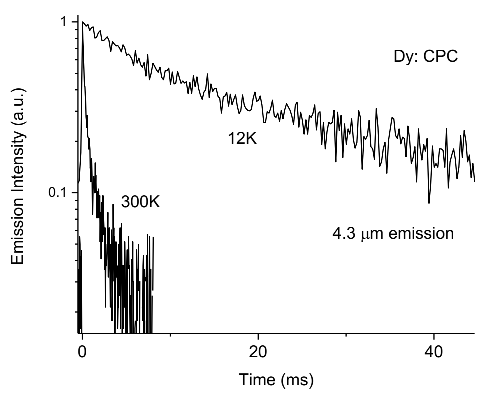


Figure 5. Mid-IR emission lifetimes at 300 K and 12 K for Dy: CPC monitored at 2.8 μm (left) and 4.3 μm (right).

The mid-IR emission lifetimes for Dy: CPC at 12 K and 300 K for the 2.8 μm and 4 μm emission bands are shown in Fig. 5. In both cases the transients were non-exponential and strongly temperature dependent. The 2.8 μm emission lifetimes (1/e decay times) were determined to be ~0.2 ms and ~10.0 ms at 300 K and 12 K, respectively. The 4.3 μm emission lifetime was ~0.4 ms at room-temperature and increased to ~14 ms at low temperature. The observed lifetime reduction with increasing temperature indicates that both mid-IR emissions are strongly quenched at room temperature. Based on predictions by the energy-gap law, significant multi-phonon relaxations are expected for the ~4.3 μm emission assuming a maximum phonon energy of $h\omega \sim 375$ $cm^{-1}$ [12] and using host-dependent phenomenological parameters for a crystal with similar phonon-energy (e.g. $LaF_3$, $h\omega_{max} \sim 350$ $cm^{-1}$) [9]. The 2.8 μm emission, however, is expected to be dominantly radiative at room-temperature, which suggest that concentration effects and possible OH quenching could play a significant role. Assuming that the measured 12K lifetimes are purely radiative, the peak emission cross-sections were estimated to be $\sim 1.3 \times 10^{-20}$ $cm^2$ and $0.2 \times 10^{-20}$ $cm^2$ for the 2.8, and 4.3 μm emission bands, respectively. More detailed studies on the mid-IR emissions from Dy: CPC are still in progress.

## 4. SUMMARY

The material preparation and IR spectroscopy of Dy doped TPB and CPC crystals grown by vertical Bridgman technique were presented. The resulting Dy: TPB crystal was of good optical quality and characteristic $Dy^{3+}$ IR absorption bands were determined to perform a Judd-Ofelt analysis. Based on JO-analysis and temperature dependent lifetime studies it was concluded that the 2.85 and 4.33 μm emission efficiencies were near unity at room temperature. On the other hand, the weaker 5.41 μm emission band was quenched most likely due to multi-phonon relaxations and upconversion processes. The synthesized Dy: CPC material was of significantly lower quality with poor transmission. Mid-IR emissions in the ~2.8, ~4.3 μm regions were observed at room temperature with strongly quenched emission lifetimes. Materials studies to improve the optical quality of Dy: CPC are in progress to further evaluate this crystal for IR photonics.


## ACKNOWLEDGEMENTS

The work at Hampton University was supported by the National Science Foundation through grant NSF-DMR 1827820 (PREM) and the Army Research Office through grant W911NF1810447.


## REFERENCES


[1] R. Babu, L. Giribabu, S. P. Singh, "Recent Advances in Halide-Based Perovskite Crystals and Their Optoelectronic Applications", Cryst. Growth Des. 18 (4), 2645 (2018).

[2] H.H. Ma, M. Imran, Z. Dang, and Z. Hu; "Growth of Metal Halide Perovskite, from Nanocrystal to Micron-Scale Crystal: A Review"; Crystals, 8, 182 (2018).

[3] Y. Zhou, J. Chen, O. M. Bakr, H. Sun, "Metal-doped lead halide perovskites: synthesis, properties, and optoelectronic applications", Chem. Mater. 30, 6589-6613 (2018).

[4] M. C. Nostrand, R. H. Page, S.A. Payne, L. I. Isaenko, and A. P. Yelisseyev, "Optical Properties of $Dy^{3+}$ and $Nd^{3+}$ doped $KPb_2Cl_5$," J. Optical Society of America B, 18, 264 (2001).

[5] S. R. Bowman, S. K. Searles, N. W. Jenkins, S.B. Qadri, E.F. Skelton, J. Ganem, in: C. Marshal (Ed.), Trends in Optics and Photonics, Advanced Solid State Lasers, 50 Optical Society of America, Washington, DC, p. 154 (2001).

[6] A. G. Okhrimchuk, L. N. Butvina, E. M Dianov, I. A. Shestakova, N. V. Lichkova, V. N. Zagorodney, A. Shestakov, "Optical spectroscopy of the $RbPb_2Cl_5$: $Dy^{3+}$ laser crystal and oscillation at 5.5 μm at room temperature", J. Opt. Soc. Am. B 24, 2690 (2007).

[7] E. E. Brown, A. G. Bluiett, U. Hommerich, A. Simmons, S. B. Trivedi, W. L. Boncger, M. P. Hehlen, A Lindey, M. Zhuravleva, "Optical spectroscopy of rare-earth doped ternary lead based halides, Opt. Mat. 7, 4415 (2017).

[8] U. Hommerich, E. Brown, A. Kabir, D. Hart, S. B. Trivedi, F. Jin, H. Chen, "Crystal growth and characterization of undoped and Dy-doped $TlPb_2Br_5$ for infrared lasers and nuclear radiation detection", J. Cryst. Growth, 479, 89 (2017).

[9] A. A. Kaminskii, *Crystalline lasers: Physical processes and operating schemes*, CRC press, New York (1996).

[10] K. Rademaker, W. F. Krupke, R. H. Page, S. A. Payne, K. Petermann, G. Huber, L. Isaenko, and U. N. Roy, A. Burger. K. Nitsch, "Optical properties of $Nd^{3+}$- and $Tb^{3+}$-doped $KPb_2Br_5$ and $RPb_2Br_5$ with low nonradiative decay", J. Opt. Soc. Am. B 21, 2117 (2004).

[11] H. U. Güdel, M. Pollnau, "Near infrared to visible photon upconversion processes in lanthanide doped chloride, bromide, and iodide lattices", J. Alloys and Comp. 303-304, 307 (2000).

[12] D. M. Calistru, L. Mihut, S. Lefrant, I. Baltog, "Identification of the symmetry of phonon models in $CsPbCl_3$ in phase IV by Raman and resonance-Raman scattering", J. Appl. Phys. 82, 5391 (1997).